

Relativistic three-body scattering and the $D^0 D^{*+} - D^+ D^{*0}$ system

Xu Zhang (张旭)
Institute of Theoretical physics

Based on : Xu Zhang, arXiv : 2402.02151

第七届强子谱和强子结构研讨会
4月29, 2024 成都

Outlines

- ❖ Relativistic three-body scattering
- ❖ The $D^0 D^{*+} - D^+ D^{*0}$ scattering
- ❖ Analytic structure of the $D^0 D^{*+} - D^+ D^{*0}$ scattering amplitude
- ❖ The $D^0 D^0 \pi^+$ decay and the pole position

Three-body interaction

❖ Three-body bound state

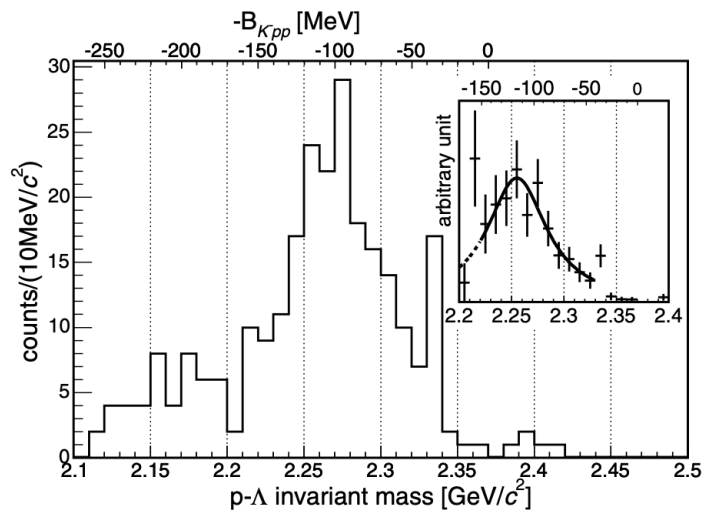
- Triton 3H
- $K^- pp$ bound state

❖ Three-body decay

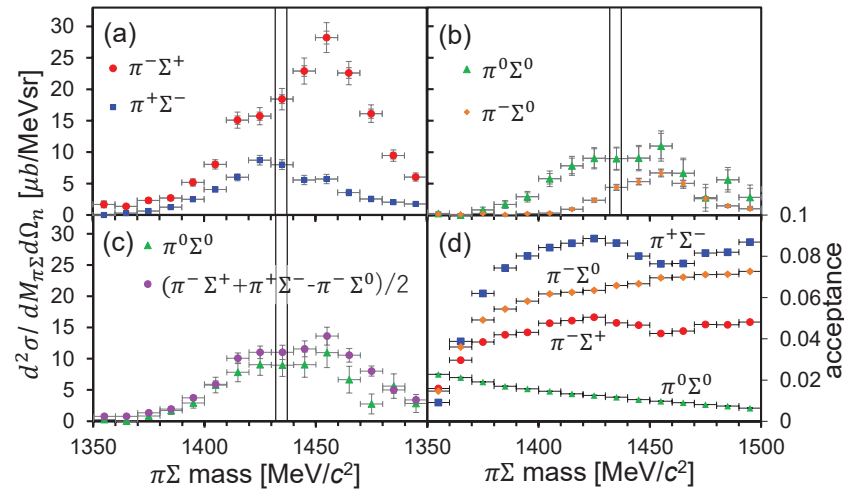
- $\pi_1(1600) \rightarrow 3\pi$
- $a_1(1260) \rightarrow 3\pi$
- $a_1(1420) \xrightarrow{?} K\bar{K}\pi$

❖ Other three-body processes

e.g. $\Lambda(1405)$ in Kd scattering



FINUDA PRL 94, 212303 (2005)



J-PARC PLB 837, 137637 (2023)
3

Relativistic three-body scattering

- ❖ Two-body subsystem interaction

R. Aaron et al., PR 174, 2022 (1968).

R. Aaron et al., Modern three-hadron physics, 1977.

A Feynman diagram showing a two-body subsystem interaction. It consists of two black lines meeting at a vertex, which is connected to a red horizontal line. The red line has a small black dot on it. This is followed by an equals sign, then another Feynman diagram where the red line is now straight, and a plus sign. Following this is a third Feynman diagram where the red line is straight and passes through a red circle containing the Greek letter Σ , with a plus sign after it. This is followed by an ellipsis (...).

→
$$A = \frac{v^\dagger v}{\sigma - m^2 - \Sigma(\sigma) + i\varepsilon}$$

Relativistic variable

- ❖ Three-body interaction

Three Feynman diagrams representing different contributions to the three-body interaction. The first diagram shows a two-body subsystem interaction (red line with a dot) coupled to a three-body system (two black lines meeting at a vertex). The second diagram shows a three-body system with a loop (red circle) coupled to a two-body subsystem interaction. The third diagram shows a two-body subsystem interaction coupled to a three-body system with a loop. These are followed by a plus sign, then a fourth diagram showing a three-body system with two loops (two red circles), followed by a plus sign and an ellipsis (...). A green arrow points to the equation below.

→
$$T = V + V \tau T$$

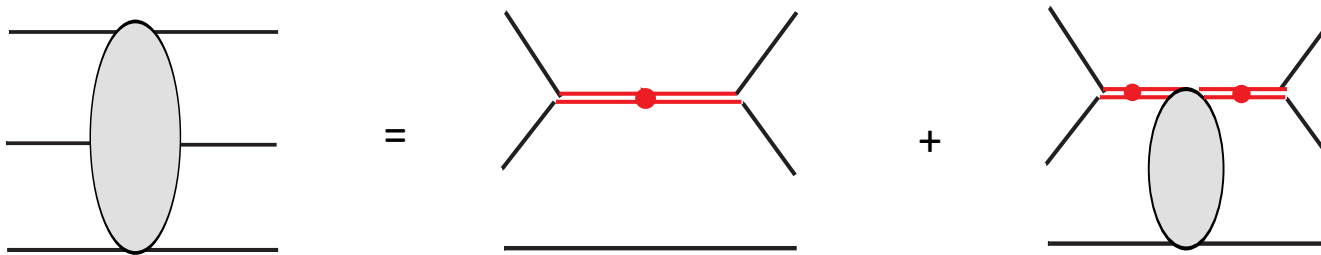
Relativistic vs non-relativistic
Different ultraviolet behavior

X. Zhang, C. Hanhart, U.-G. Meißner, and J.-J. Xie,
EPJA 58, 20 (2022).

where $\tau = \frac{1}{\sigma - m^2 - \Sigma(\sigma) + i\varepsilon}$, V is the Bonn potential.

Relativistic three-body scattering

- ❖ Three-body interaction



R. Aaron et al., PR 174, 2022 (1968).

R. Aaron et al., Modern three-hadron physics, 1977.

- ❖ Unitarity relation

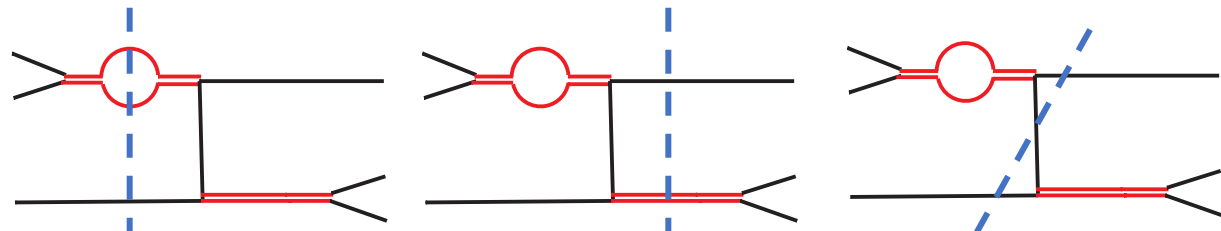
$$i [M^\dagger - M] = M^\dagger M \quad \text{green arrow}$$



$$\Sigma \sim \int_0^\infty \text{cof.} \frac{k^2 dk}{\sigma - [\varpi_D(k) + \varpi_\pi(k)]^2 + i\varepsilon}$$

- ❖ Multi-Riemann sheet

$$T(s, p', p) = V(s, p', p) + \int_0^\Lambda \frac{k^2 dk}{(2\pi)^3 2\varpi(k)} V(s, p', k) \tau(\sigma_k) T(s, k, p)$$



- Two-body unitarity cut
- Three-body unitarity cut

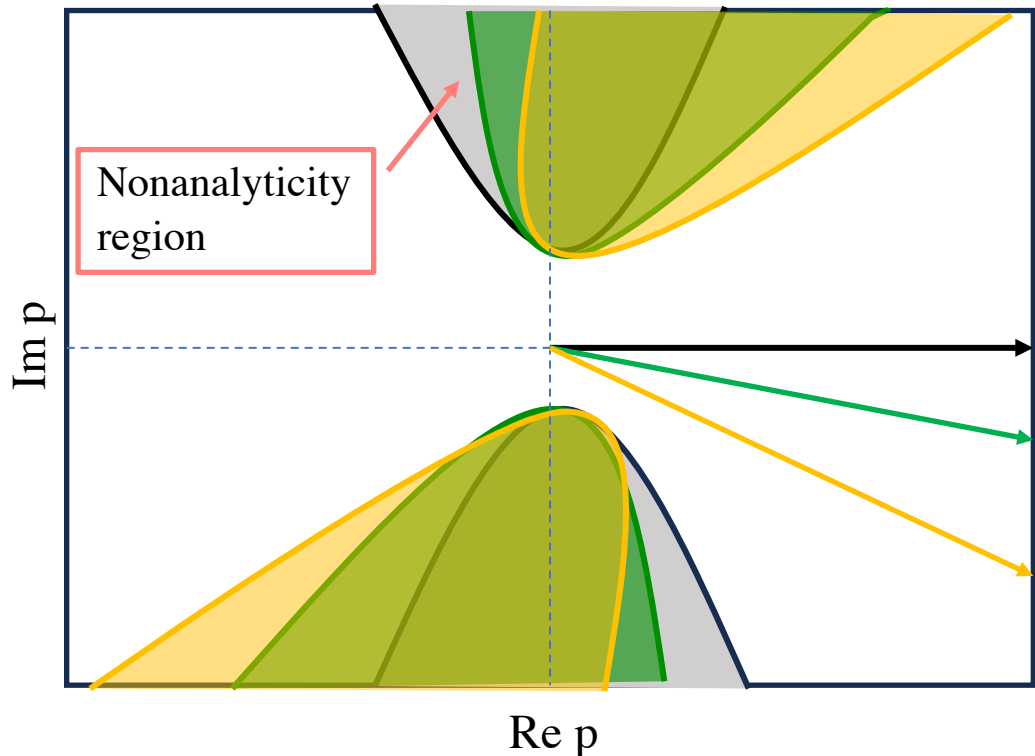
Relativistic three-body scattering

- The domains of nonanalyticity

$$V(p', p) \sim$$

$$\int_{-1}^1 \frac{dx}{\sqrt{s} - [\omega_D(p') + \omega_D(p) + \omega_\pi(q)] + i\varepsilon}$$

Denominator
= 0 → Nonanalyticity
region



- Contour deformation

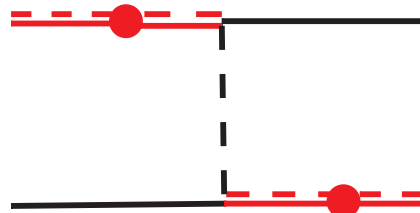
$$\begin{aligned} p &\rightarrow p e^{-i\theta} \\ p' &\rightarrow p' e^{-i\theta} \end{aligned}$$

W. Glockle, PRC 18, 564 (1978).

The analytic region is extended to the unphysical region.

D D^{}* scattering

❖ π-exchange

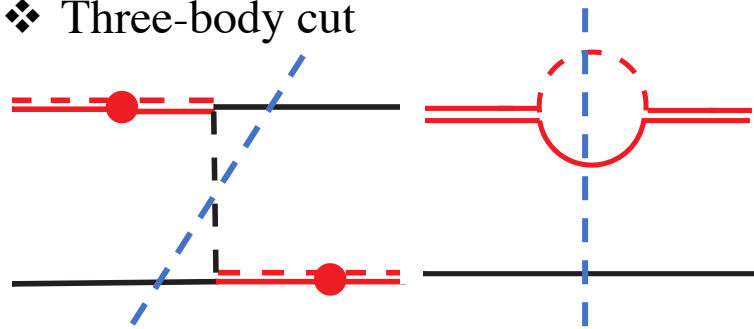


$$V \sim \frac{1}{q^2 - m_\pi^2 + i\epsilon}$$

$$q^2 - m_\pi^2 \simeq -2m_\pi\Delta + \left(1 + \frac{m_\pi^2}{4m_D m_{D^*}}\right)q$$

$$\Delta = m_{D^*} - m_D - m_\pi$$

❖ Three-body cut



Different from the NN scattering

Similar phenomenon happens in $D\bar{D}^*$

S. Fleming, M. Kusunoki, T. Mehen, and U. van Kolck, PRD 76, 034006 (2007).

M. Suzuki, PRD 72, 114013 (2005).

V. Baru, A. A. Filin, C. Hanhart, Y. S. Kalashnikova, A. E. Kudryavtsev, and A. V. Nefediev, PRD 84, 074029 (2011).

M. Schmidt, M. Jansen, and H. W. Hammer, PRD 98, 014032 (2018).

Three-body dynamics

- M.-L. Du, V. Baru, X.-K. Dong, A. Filin, F.-K. Guo, C. Hanhart, A. Nefediev, J. Nieves, and Q. Wang, PRD 105, 014024 (2022).
 L. Qiu, C. Gong, and Q. Zhao, PRD 109, 076016 (2024).
 J.-Z. Wang, Z.-Y. Lin, and S.-L. Zhu, PRD 109, L071505 (2024).

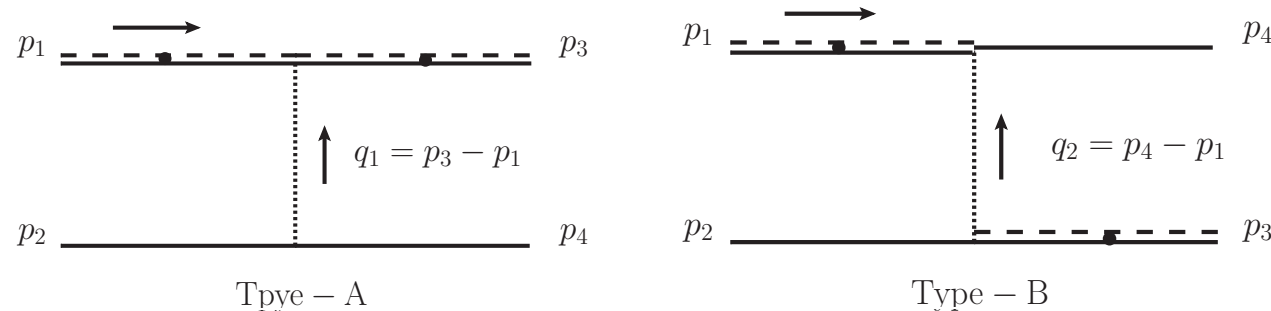
DD^* scattering

❖ Scattering equation

$$T(s, p', p) = V(s, p', p) + \int_0^\Lambda \frac{k^2 dk}{(2\pi)^3 2\omega(k)} V(s, p', k) \tau(\sigma_k) T(s, k, p)$$

$$\sigma_k = s - 2\sqrt{s}\omega_D(k) + m_D^2$$

The interaction potential (including the π , σ , ρ and ω -exchange).



The isospin factors

	Type-A			Type-B				
	ρ^0	ρ^\pm	ω	ρ^0	ρ^\pm	ω	π^0	π^\pm
1→ 1								
2→ 2	1/2	...	-1/2	...	1	1
1→ 2	...	-1	...	-1/2	...	1/2	-1/2	...

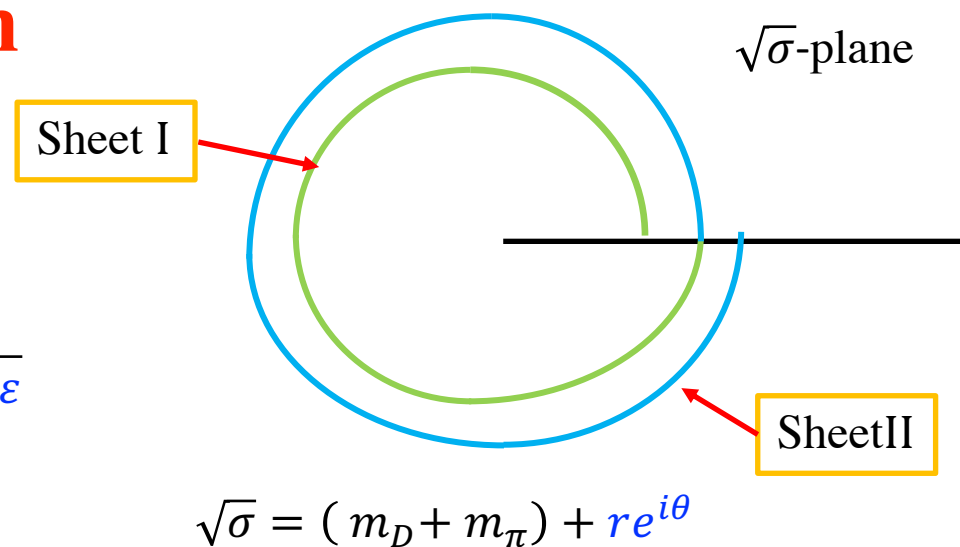
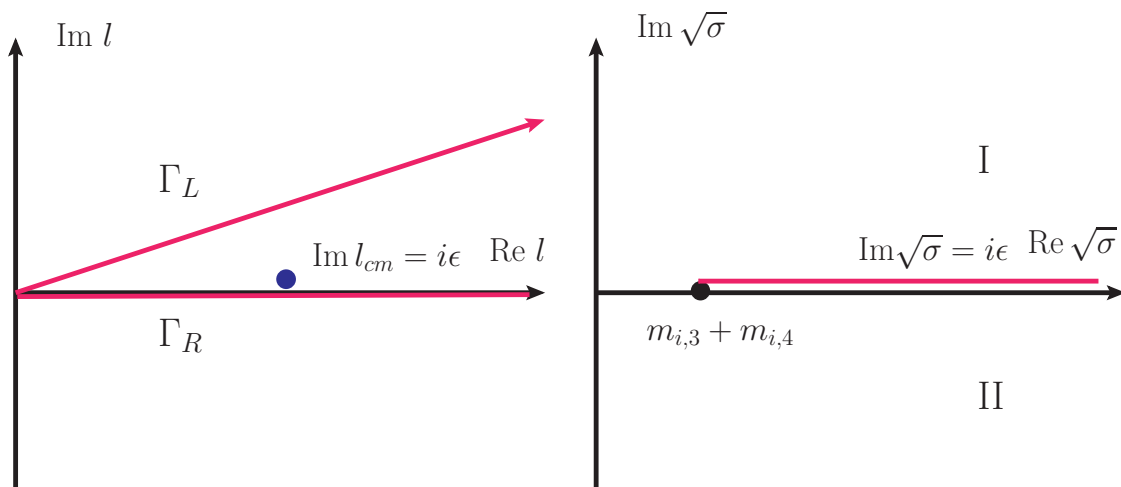
Analytic continuation

- ❖ Self-energy

- First Riemann sheet

$$\Sigma \sim \int_0^\infty cof. \frac{k^2 dk}{\sigma - [\varpi_D(k) + \varpi_\pi(k)]^2 + i\varepsilon}$$

Integral contour



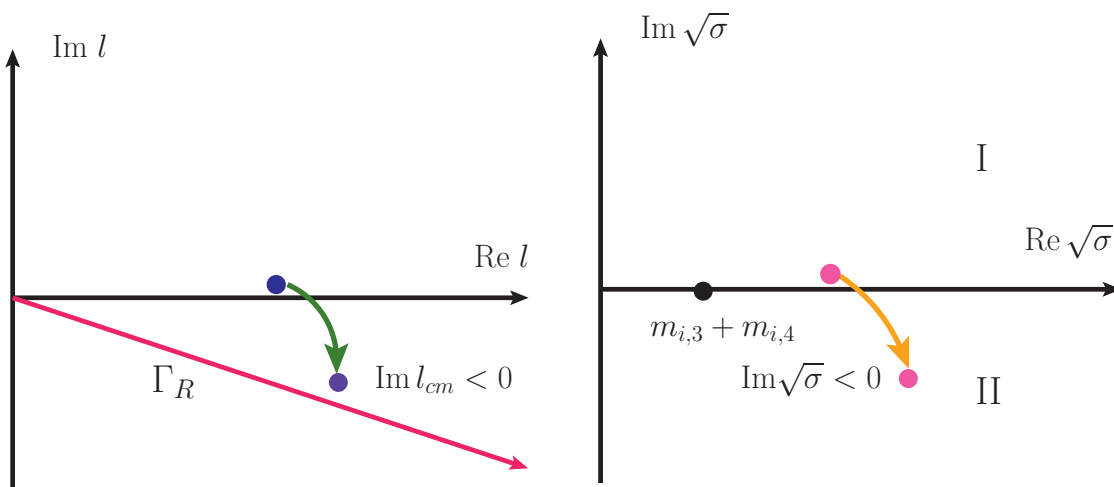
Analytic continuation

❖ Self-energy

$$\Sigma \sim \int_0^\infty cof. \frac{k^2 dk}{\sigma - [\varpi_D(k) + \varpi_\pi(k)]^2 + i\varepsilon}$$

- Second Riemann sheet (resonance)

Integral contour

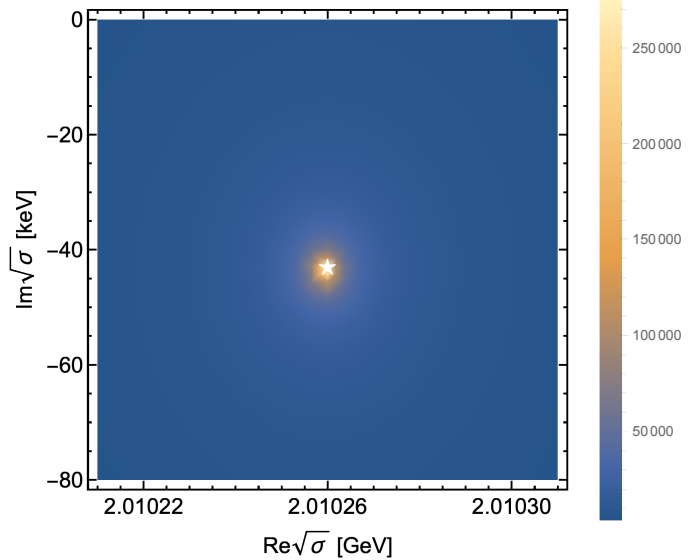


$$\tau = \frac{1}{\sigma - m^2 - \Sigma_1^R(\sigma) - \Sigma_2^R(\sigma) + i\varepsilon}$$

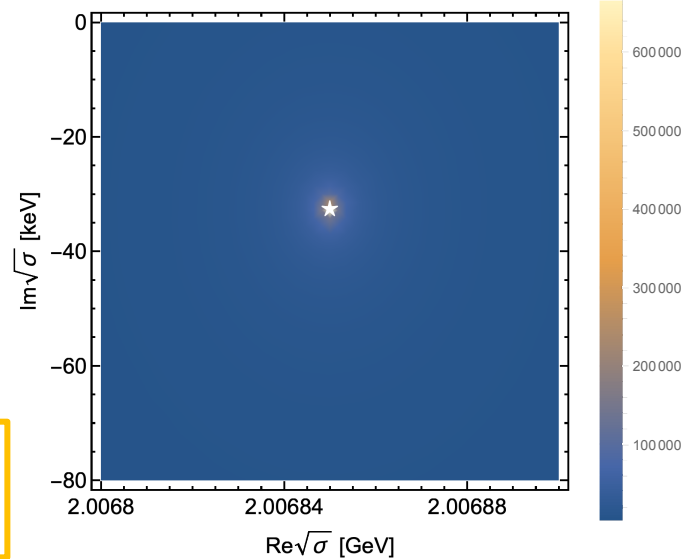
$$\Sigma_i^R(\sigma) = \Sigma_i(\sigma) - \Sigma_1^{\text{sub}}(\sigma)$$

**Dπ interaction in p-wave
Twice subtraction**

D^{*+} pole position



D^{*0} pole position

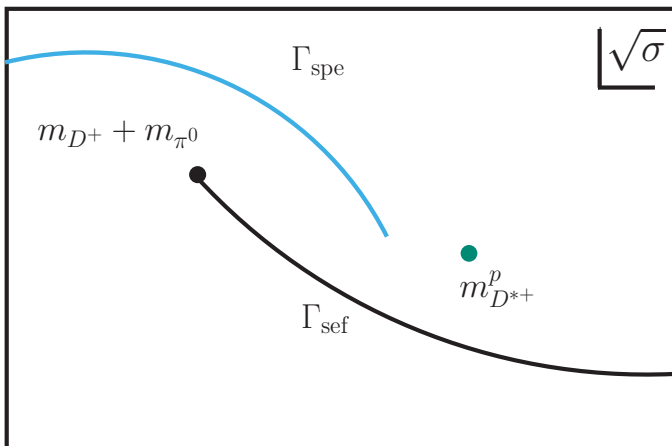
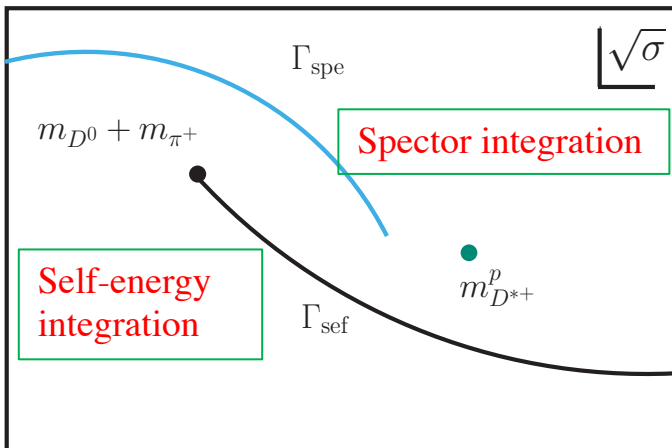


Analytic continuation

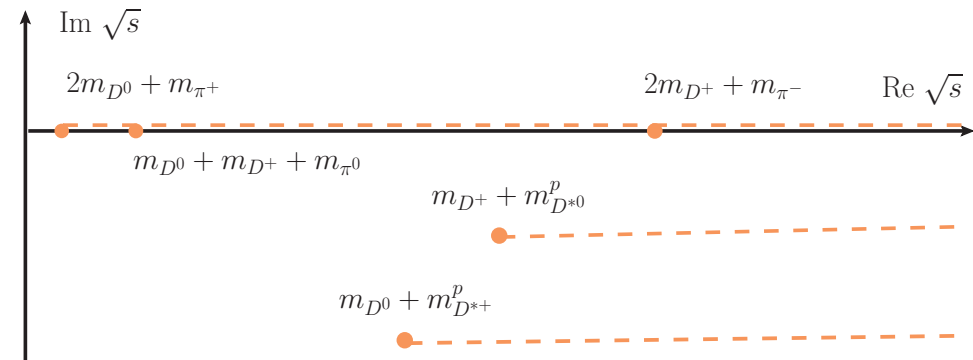
$$T(s, p', p) = V(s, p', p) + \int_0^\Lambda \frac{k^2 dk}{(2\pi)^3 2\varpi(k)} V(s, p', k) \tau(\sigma_k) T(s, k, p)$$

❖ Across the three-body cuts

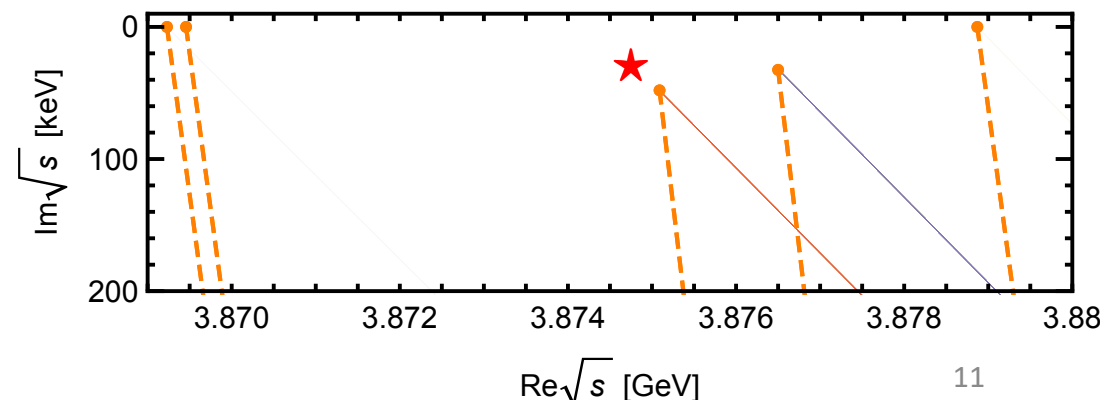
- Contour mapped in the $\sqrt{\sigma}$ plane.



- The cut structure in complex \sqrt{s} plane

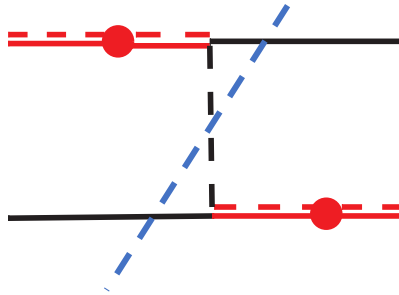


- The cut structure after contour deformation



Solution for real momentum

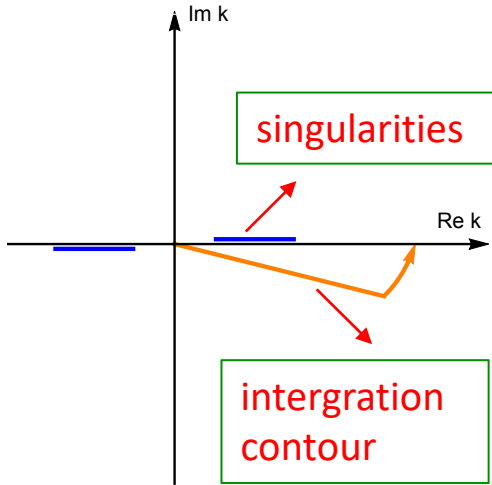
- ❖ Three-body singularities



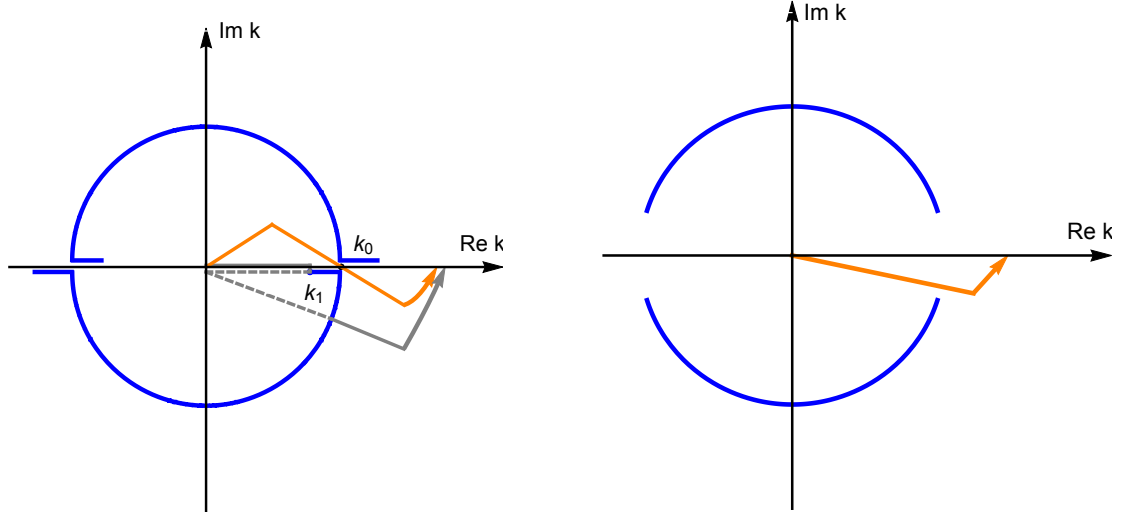
X. Zhang, H.-L. Fu, F.-K. Guo, and H.-W. Hammer,
PRC 108, 044304

$$V \sim \int_{-1}^1 \frac{dx}{\sqrt{s} - [\omega_D(p') + \omega_D(p) + \omega_\pi(q)] + i\varepsilon} \rightarrow \text{Zero}$$
$$x = \vec{p} \cdot \vec{p}' / pp'$$

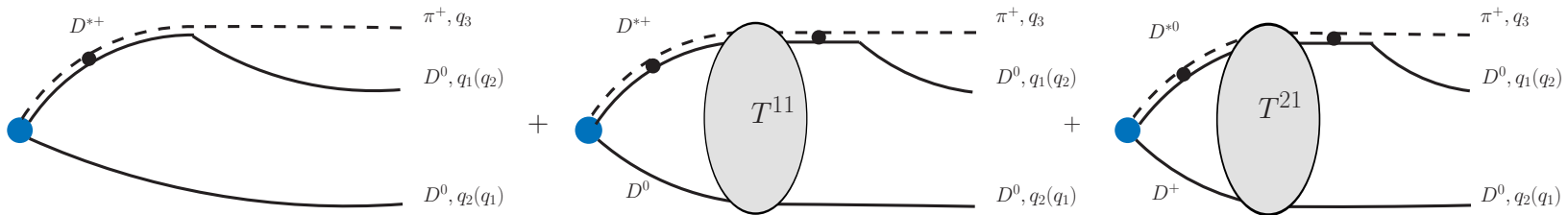
- ❖ Contour deformation



E. Schmid, H. Ziegelmann, The Quantum Mechanical Three-Body Problem



Three-body $D^0 D^0 \pi^+$ decay



- ❖ The mass distribution

$$\frac{d\Gamma(\sqrt{s})}{d\sqrt{s}} = \int \frac{1}{(2\pi)^5} \frac{1}{16s} \left(\frac{1}{3} \sum_{\Lambda} |\sum_{\lambda} M_{\Lambda\lambda}(\vec{q}_1, \vec{q}_2, \vec{q}_3)|^2 \right) q_3^* q_1 dm_{23} d\Omega_3^* d\Omega_1$$

Decay amplitude

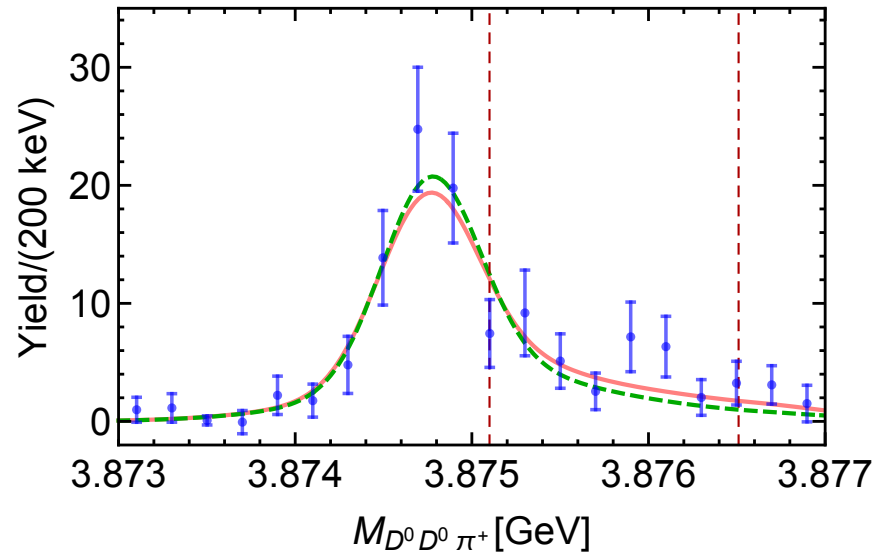
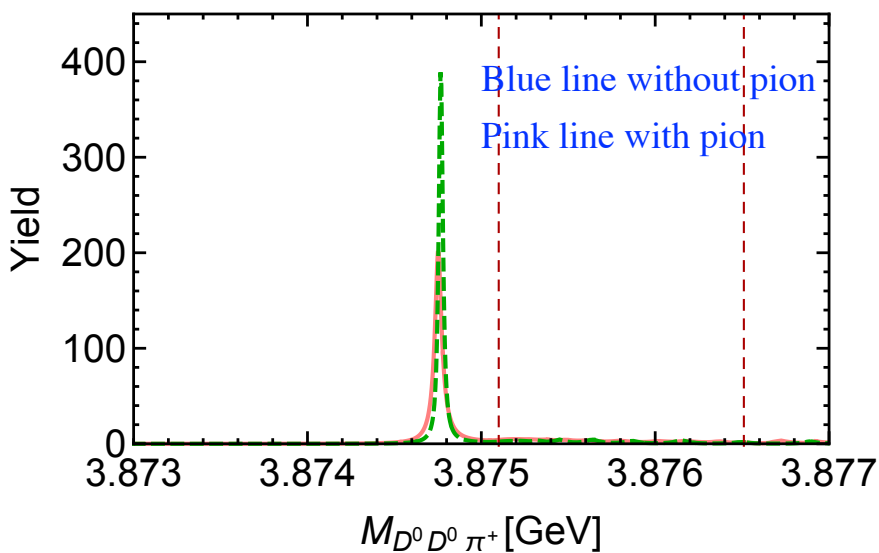
$$M_{\Lambda\lambda}(\vec{q}_1, \vec{q}_2, \vec{q}_3) = \frac{\mathcal{F}}{\sqrt{2}} \left[\sqrt{\frac{3}{4\pi}} D_{\Lambda\lambda}^{1*}(\phi_1, \theta_1, 0) \textcolor{blue}{M_L(q_1)} U_{L\lambda} v_{\lambda}(\vec{q}_2, \vec{q}_3) + \vec{q}_1 \leftrightarrow \vec{q}_2 \right]$$

- ❖ Short-distance interaction is absorbed into \mathcal{F} .

Numerical results

Cut off Λ and the pole positions from fitting of the $D^0 D^0 \pi^+$ line shape obtained by the LHCb Collaboration.

Scheme	$\chi^2/d. o. f$	Λ GeV	$\sqrt{s_{pole}^{thr}}$ keV
I	$18.11/(20-1) = 0.95$	0.4551 ± 0.0018	$-332^{+37}_{-36} - i(18 \pm 1)$
II	$14.47/(20-1) = 0.76$	0.3701 ± 0.0017	$-351^{+37}_{-35} - i(28 \pm 1)$



Fitting results of the $D^0 D^0 \pi^+$ line shapes before (left panel) and after (right panel) convolution with the energy resolution function.

Summary

- ❖ The analytic continuation of the coupled-channel $D^0 D^{*+} - D^+ D^{*0}$ scattering amplitude is studied.
- ❖ The π -exchange term has a signification on the pole position of the T_{cc}^+ . Including the π -exchange term, the width of T_{cc}^+ will be increased by a factor of 1.5.
- ❖ We will extend our framework to calculate $3\pi - K\bar{K}\pi$ coupled system.

Thank you for your attention!